

# UC Irvine

## UC Irvine Previously Published Works

### Title

Deep learning-based muscle segmentation and quantification at abdominal CT: application to a longitudinal adult screening cohort for sarcopenia assessment

### Permalink

<https://escholarship.org/uc/item/0c75m088>

### Journal

British Journal of Radiology, 92(1100)

### ISSN

0007-1285

### Authors

Graffy, Peter M  
Liu, Jiamin  
Pickhardt, Perry J  
et al.

### Publication Date

2019-08-01

### DOI

10.1259/bjr.20190327

Peer reviewed

Received:  
02 April 2019Revised:  
31 May 2019Accepted:  
12 June 2019<https://doi.org/10.1259/bjr.20190327>

Cite this article as:

Graffy PM, Liu J, Pickhardt PJ, Burns JE, Yao J, Summers RM. Deep learning-based muscle segmentation and quantification at abdominal CT: application to a longitudinal adult screening cohort for sarcopenia assessment. *Br J Radiol* 2019; **92**: 20190327.

## FULL PAPER

# Deep learning-based muscle segmentation and quantification at abdominal CT: application to a longitudinal adult screening cohort for sarcopenia assessment

<sup>1</sup>PETER M. GRAFFY, <sup>2</sup>JIAMIN LIU, <sup>1</sup>PERRY J. PICKHARDT, <sup>3</sup>JOSEPH E. BURNS, <sup>2</sup>JIANHUA YAO and <sup>2</sup>RONALD M. SUMMERS

<sup>1</sup>University of Wisconsin School of Medicine and Public Health 600 Highland Avenue, Madison, WI 53705,

<sup>2</sup>Radiology and Imaging Sciences, National Institutes of Health Clinical Center, 10 Center Drive, Bethesda, MD 20892-1182

<sup>3</sup>Department of Radiological Sciences, University of California-Irvine, Orange, CA

Address correspondence to: Dr Perry J. Pickhardt

E-mail: [ppickhardt2@uwhealth.org](mailto:ppickhardt2@uwhealth.org)

**Objective:** To investigate a fully automated abdominal CT-based muscle tool in a large adult screening population.

**Methods:** A fully automated validated muscle segmentation algorithm was applied to 9310 non-contrast CT scans, including a primary screening cohort of 8037 consecutive asymptomatic adults (mean age, 57.1±7.8 years; 3555M/4482F). Sequential follow-up scans were available in a subset of 1171 individuals (mean interval, 5.1 years). Muscle tissue cross-sectional area and attenuation (Hounsfield unit, HU) at the L3 level were assessed, including change over time.

**Results:** Mean values were significantly higher in males for both muscle area (190.6±33.6 vs 133.3±24.1 cm<sup>2</sup>,  $p<0.001$ ) and density (34.3±11.1 HU vs 27.3±11.7 HU,  $p<0.001$ ). Age-related losses were observed, with mean muscle area reduction of -1.5 cm<sup>2</sup>/year and attenuation reduction of -1.5 HU/year. Overall age-related muscle density (attenuation) loss was steeper than for muscle area for both sexes up to the age of 70 years. Between ages 50 and 70, relative muscle attenuation decreased significantly more in females (-30.6% vs -18.0%,  $p<0.001$ ),

whereas relative rates of muscle area loss were similar (-8%). Between ages 70 and 90, males lost more density (-22.4% vs -7.5%) and area (-13.4% vs -6.9%,  $p<0.001$ ). Of the 1171 patients with longitudinal follow-up, 1013 (86.5%) showed a decrease in muscle attenuation, 739 (63.1%) showed a decrease in area, and 1119 (95.6%) showed a decrease in at least one of these measures.

**Conclusion:** This fully automated CT muscle tool allows for both individualized and population-based assessment. Such data could be automatically derived at abdominal CT regardless of study indication, allowing for opportunistic sarcopenia detection.

**Advances in knowledge:** This fully automated tool can be applied to routine abdominal CT scans for prospective or retrospective opportunistic sarcopenia assessment, regardless of the original clinical indication. Mean values were significantly higher in males for both muscle area and muscle density. Overall age-related muscle density (attenuation) loss was steeper than for muscle area for both sexes, and therefore may be a more valuable predictor of adverse outcomes.

## INTRODUCTION

Sarcopenia is characterized by progressive and generalized loss of skeletal muscle mass, which often correlates with poor health and even impending death. Cachexia is a related condition characterized by extreme weight loss and muscle wasting and is a relatively common manifestation of a number of chronic diseases. Studies estimate that 5–10% of adults over 60 years of age are sarcopenic, and half of all patients with cancer progressively lose skeletal muscle mass due to cachexia.<sup>1,2</sup> Operational methods to assess muscle

loss typically involve calculation of the patient's skeletal muscle index (SMI), which can be accomplished using a variety of imaging modalities. However, neither sarcopenia nor cachexia maintain a standard definition based on a single validated measurement technique.

CT imaging is generally considered the most accurate and reliable method to assess muscle mass and density. Dual energy X-ray absorptiometry (DXA) and bioelectric impedance analysis (BIA) are currently the most commonly used

techniques due to relative cost and accessibility.<sup>2-4</sup> Nonetheless, manual, semi-automated, and automated algorithmic techniques at CT have been shown to be more accurate and robust, as muscle tissue can be easily identified, segmented, and quantified.<sup>5,6</sup> The L3 level at CT represents a preferred site for measurement, with prior work showing that this level is optimal for assessing the psoas, paraspinal, and abdominal wall musculature.<sup>5-8</sup> The development of novel fully automated measurement methods has further increased the potential value and practicality of CT imaging with regards to the detection of sarcopenia.

A wide array of semi-automated and automated quantitative CT measures have been developed within the past decade for a variety of purposes. In addition to muscle measures, we have been actively pursuing other CT-based biomarkers, including measures of bone, fat, and vascular calcification.<sup>9-11</sup> Fully automated methods potentially allow for more widespread implementation of opportunistic detection for CT scans performed for other clinical indications, which could provide a number of advantages over DXA and BIA. We are not aware of any previous studies that have investigated the utilization of a fully automated approach to characterize the population distribution and changes over time of muscle mass and density in a large, longitudinal patient cohort. The purpose of this study was to apply an automated CT-based abdominal muscle tissue segmentation algorithm to a large asymptomatic adult cohort undergoing routine CT colonography (CTC) screening to determine normal age- and gender-related differences at the population level in muscle bulk and density.

## METHODS AND MATERIALS

### Patient population

This was an IRB-compliant, HIPAA-approved retrospective cohort study. Unenhanced abdominal CT scans from 8037 asymptomatic adults who underwent initial CTC screening at a single academic medical center between April 2004 and December 2016 were anonymized and available for inclusion in this study. In total, 9582 total CT examinations were evaluated, with 272 excluded based on either algorithmic segmentation failure or other technical failures (including lack of images), yielding a final total cohort of 9310 eligible studies. A total of 1171 patients had at least one follow-up CTC study, which were included to assess for longitudinal changes over time. No patient was excluded for pathology or hardware identified on the CT scan itself. Of note, the initial cohort size differs slightly from separate investigations of other CT-based biomarkers,<sup>9-11</sup> primarily related to differences in available anonymized data sets at the time that each specific tool was evaluated.

### CT scanning protocol

Specifics relating to CTC technique such as bowel preparation and distention have been previously described and are beyond the scope or concern of this study.<sup>12</sup> Breath-hold CT acquisition of the abdomen and pelvis without i.v. contrast was obtained in both supine and prone positions, but only the former was utilized herein for muscle assessment. All CT scans were performed on 8-64 multidetector-row scanners (GE Healthcare; Waukesha, WI, USA). Detector configuration was  $8 \times 1.25$ ,  $16 \times 1.25$ , or  $64$

$\times 0.625$ . Scanning was performed at 120 kV<sub>p</sub> for all scans, with low-dose mA settings using Smart-mA with noise index set at 50 and Smart-mA range set at 30-150. Images for extracolonic evaluation were reconstructed using 5 mm slice thickness at 3 mm intervals.

### Automated algorithm for muscle tissue measurements

The muscle segmentation algorithm utilized in this study represents a fully automated deep learning system developed, trained, and tested at the NIH Clinical Center on separate CT cohorts from that investigated in the current study.<sup>13,14</sup> The CT images were first processed by fully automated spine segmentation and labeling software that identifies the slice that corresponds to the superior and inferior endplates of each vertebral body from T12-L5.<sup>13,14</sup> Volumetric slabs of the abdominal CT cross-section were obtained at each of these levels, with cranio-caudal slab thickness based on vertebral height.

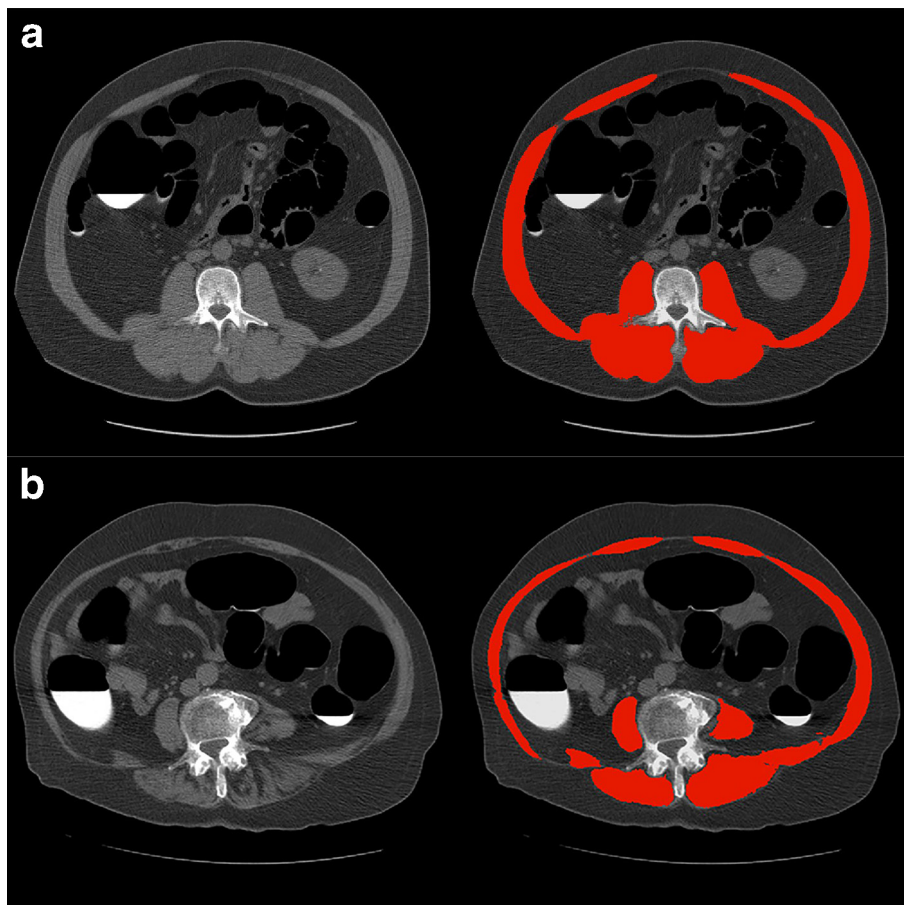
Then, the U-Net neural network model was utilized for automated detection and segmentation of muscles, due to its precise and rapid segmentation.<sup>15</sup> The U-Net is a well-known machine learning algorithm that can be taught how to segment anatomic structures and lesions on medical images. For this project, the training consisted of presenting images and manual segmentations of the muscles to the algorithm. As noted above, the training set was distinct from the data set used in this study. Cross-entropy was used for the loss function and optimization was done using "Adam's" method.<sup>14</sup> Manual muscle segmentations at two axial levels for each lumbar vertebra in the training set were used to train the model for the deep learning system. During testing, the trained model was deployed for muscle segmentations at multiple lumbar vertebral levels. Using manual segmentation as ground truth, the Dice coefficient for L3 total abdominal muscle cross-section for this fully automated tool was shown to be  $0.938 \pm 0.028$ .<sup>14</sup> Examples of the visual appearance of this segmentation and quantification is shown in [Figure 1](#), including a case without and with some degree muscular atrophy.

The automated tool provides an analysis of both muscle density and bulk at the L3 level. The L3 level represents a useful landmark for muscle measurement, as prior work has shown that this level is optimal for visualizing the psoas, paraspinal, and abdominal wall musculature.<sup>5-8</sup> Muscle density quantification is performed by calculating the average Hounsfield unit (HU) within each voxel containing muscle tissue at the L3 level. Muscle volumetric quantification is performed by multiplying muscle voxel counts by voxel volumes (*i.e.* the pixel area times the slice thickness) to get the volumes in each slab volume corresponding to T12-L5 body regions. Again, the L3 level was used for analysis. In total, the muscle tissue measurement algorithm takes less than 1 min to process an abdominal-region study (Intel Core i7 processor with 4x Nvidia Titan X GPUs and 12 GB memory per GPU).

### Statistical analysis

Summary statistics were collected for the patient population based on age and gender. The mean L3 cross-sectional muscle area (cm<sup>2</sup>) was calculated by taking muscle volume (cm<sup>3</sup>) over

Figure 1. Muscle segmentation for quantification using our automated algorithm. (a, b) Unenhanced transverse (axial) CT images at the L3 level in a 50-year-old male (a) and a 87-year-old female (b) undergoing colonography screening, both without (left) and with (right) the automated muscle segmentation depicted. In (b) note how the areas of fatty involution in the paraspinal musculature (left >right) in (b) remain segmented as muscle, which would decrease the mean attenuation value but not the area.



the L3 vertebral level and dividing it by craniocaudal slab thickness of L3 (cm). The SMI is defined as the cross-sectional muscle area at L3 in  $\text{cm}^2$  divided by the patient height in  $\text{m}^2$ .

In patients with follow-up CTC scans, changes in muscle density and area were recorded, as was change per year by dividing the amount of change in an individual patient by the numbers of years between initial and follow-up CTC. From these, percent area and density change were calculated by taking the difference in HU and area between the two scans, dividing this result by the values found on the initial CTC, and multiplying by 100. Percent change over time was calculated by taking the percent change and dividing by the interval years between scans.

Comparison of means was done using independent *t*-tests for muscle tissue between genders and ages with a null hypothesis value of 0.05. Data processing and analysis was performed using base R (R Core Team, v. 3.4.2).

## RESULTS

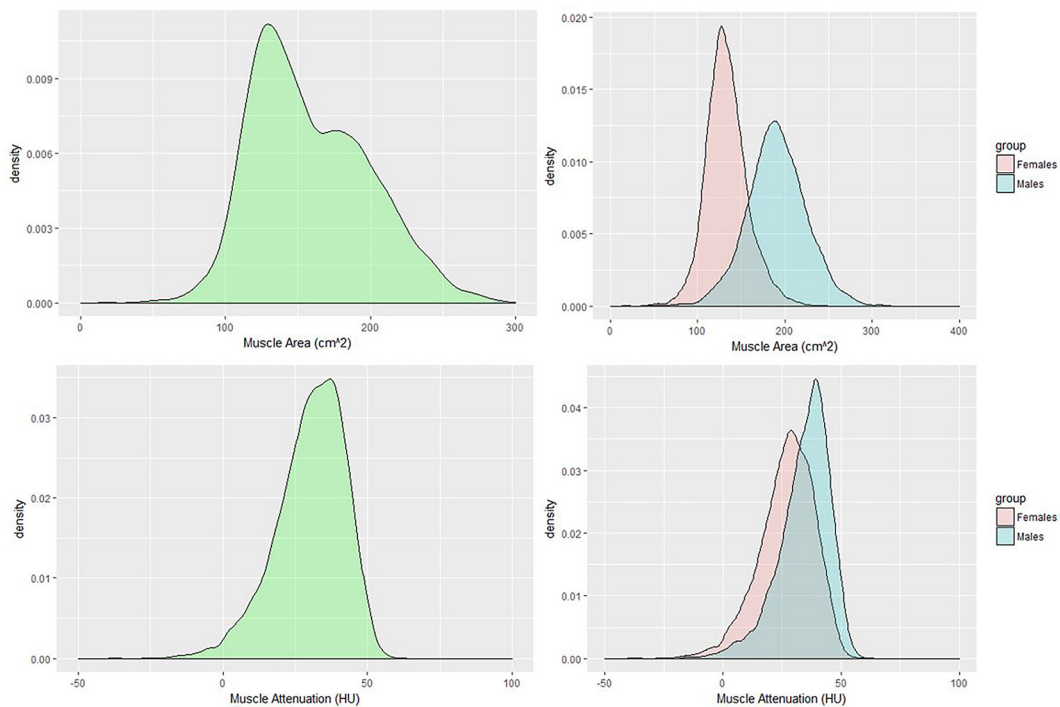
The mean age ( $\pm$ standard deviation) of the 8037 individual patients included in this study was  $57.1 \pm 7.8$  years; there were 3555 males and 4482 females. There were 1171 patients (549

males and 622 females) with a follow-up study (mean interval, 5.1 years).

Both muscle bulk and density at CT (in terms of L3 cross-sectional area and attenuation in HU, respectively) were found to have relatively normal distributions among the entire asymptomatic adult population, as well as among each gender (Figure 2). For muscle density, some skew was seen towards lower attenuation values. Mean values for muscle cross-sectional area and attenuation according to age and gender are shown in Figure 3 and Table 1. Overall, males were found to have significantly higher muscle area ( $190.6$  vs  $133.3$   $\text{cm}^2$ ,  $p < 0.001$ ) and density ( $34.3$  HU vs  $27.3$  HU,  $p < 0.001$ ) compared with females. This yielded a higher SMI for males ( $60.2$  vs  $49.8$   $\text{cm}^2/\text{m}^2$ ) as well.

As age increased, muscle area and density progressively decreased over time for both sexes combined (Figure 3A) and also when considered separately (Figure 3B). From the ages of 40 to  $-90$  years, males lost  $62.9$   $\text{cm}^2$  (32.2%) of muscle area, while females lost  $21.4$   $\text{cm}^2$  (21.4%). Both sexes lost approximately 67% of muscle density during the same 50 year span. Between ages 50 and 70, relative muscle density decreased significantly more for females than males ( $-30.6\%$  vs  $-18.0\%$ ,  $p < 0.001$ ), whereas

Figure 2. Density plots of muscle cross-sectional area (top row) and attenuation (bottom row) at the L3 level of the entire study cohort ( $n = 8037$ ) combined (left images) and according to gender (right). Note the bimodal normal distribution of L3-level muscle area for males and females, with greater values in the former. For muscle attenuation, both gender distributions skew to lower values but otherwise appear normally distributed, with less gender separation.



rates of muscle area loss were similar, at approximately  $-8\%$ . However, between ages 70 and 90, males lost significantly more muscle density ( $-22.4\%$  vs  $-7.5\%$ ) and area ( $-13.4\%$  vs  $-6.9\%$ ) ( $p < 0.001$ ). As shown in Figure 1, the increased loss of muscle attenuation compared with muscle area as patients age may relate to how atrophic muscle with partial fatty change remains segmented as muscle (hence, attenuation would decrease more than area loss).

Of the 1171 patients with longitudinal CT follow-up (mean interval, 5.1 years), 1013 (86.5%) showed a decrease in muscle attenuation, 739 (63.1%) showed a decrease in area, and 1119 (95.6%) showed a decrease in at least one of these measures. Again, the greater loss of muscle attenuation over area likely reflects the fact that the muscle remains segmented (Figure 1B). During the follow-up interval, males and females on average lost

Figure 3. Muscle area and attenuation differences according to subject age. (a) Graph shows mean CT-based muscle cross-sectional area (blue line) and attenuation (red line) at the L3 level according to age. Note that muscle density (measured by HU attenuation values) decreases at a greater rate than muscle area. (b) Graph shows mean CT-based muscle cross-sectional area (dotted lines) and attenuation (solid lines) according to both age and gender (males in blue, females in yellow). Despite male-female offset in mean values, the overall trends appear similar for ages 40-70 years. After age 70, female attenuation and area values plateau more than males.

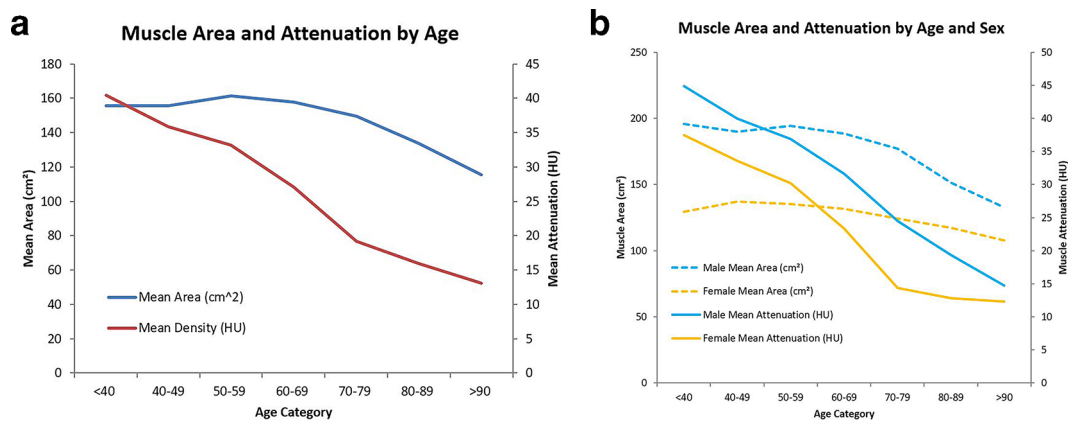


Table 1. Aggregate data for CT-based muscle area and attenuation at the L3 level by gender

	Male (n = 4161)			Female (n = 5149)			p
	Mean	SD	Median	Mean	SD	Median	
Age (Years)	58.08	7.80	57.00	57.51	7.74	56.00	0.0004
BMI (kg/m <sup>2</sup> )	29.27	5.35	28.40	28.52	8.56	26.90	<0.0001
Muscle area (cm <sup>2</sup> )	190.61	33.69	189.92	133.32	24.11	131.38	<0.0001
Muscle attenuation (HU)	34.34	11.08	36.14	27.30	11.69	28.07	<0.0001
SMI	60.18	10.97	59.87	49.79	9.38	48.94	<0.0001

BMI, body mass index; HU, Hounsfield unit; SD, standard deviation; SMI, skeletal muscle index.

muscle density at a similar rate ( $-1.5$  HU/year vs  $-1.4$  HU/year) and overall quantity (mean loss,  $-7.1$  HU vs  $-7.5$  HU). However, males lost muscle area at a significantly higher mean annual rate than females ( $-2.2$  vs  $-0.91$  cm<sup>2</sup>/year) and mean quantity ( $-7.9$  vs  $-4.4$  cm<sup>2</sup>,  $p < 0.001$ ) during the follow-up interval. As shown in Table 2, males also had comparable interquartile ranges to females for density, but had greater interquartile ranges for area loss.

Using previously published SMI-based thresholds for sarcopenia of 45.4 cm<sup>2</sup>/m<sup>2</sup> in males and 34.4 cm<sup>2</sup>/m<sup>2</sup> in females<sup>16</sup>, we found an overall sarcopenia prevalence of 5.2%. The prevalence was 7.6% in males and 3.2% in females. Among patients with follow-up scans, 1.3% developed interval sarcopenia by crossing below this threshold.

Exclusions ( $n = 272$ ) were primarily due to missing or incorrect DICOM series. In a small subset of cases, L3 segmentation failure occurred, most often resulting from artifacts related to various combinations of metallic implants, compression fractures, patient motion, and low-dose technique (Figure 4). The final technical failure rate related to segmentation was 0.28%.

## DISCUSSION

Given our relatively unique abdominal cohort of asymptomatic and relatively healthy outpatient adults, our study provides useful normative values for abdominal muscle area and attenuation at

CT, including age- and gender-related differences. In addition, we demonstrate the potential utility of the fully automated muscle segmentation algorithm that we employed. To our knowledge, this retrospective cohort study is the first to achieve fully automated muscle segmentation measurements on a large asymptomatic screening population. With the information and CT tool provided by this study, clinicians and researchers can potentially evaluate sarcopenia and cachexia in adults on any unenhanced abdominal CT scan, either prospectively or retrospectively. We hope to validate its use on CT scans performed with i.v. contrast in the near future. The calculated prevalence of sarcopenia using this fully automated algorithm compares favorably in relation to previous reports using manual measurements, especially given that our mean population age is less than 60 years of age.<sup>16</sup>

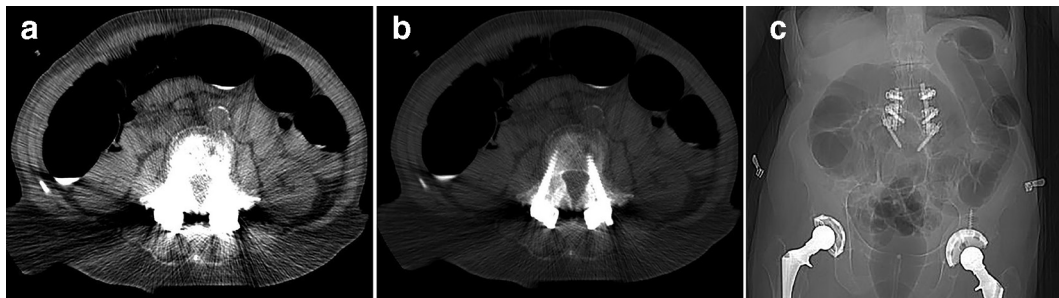
This study found mean muscle cross-sectional area and attenuation to be significantly different for males and females, as well as the rates of change over time. The greater loss of muscle density (attenuation) compared with muscle bulk (area) may reflect the fact that fatty muscle was often still segmented, which would lower HU over area. Adult males had approximately 30% more abdominal muscle and 20% more muscle attenuation than females on average. While both sexes lost muscle density (as measured by HU attenuation) at about the same rate, males lost significantly more muscle area than females between the ages of 40 and 90, especially between 70 and 90. This demonstrates that males start with more muscle mass overall but lose it at a faster

Table 2. Inpatient changes in muscle measurements for the subcohort with follow-up scans

	Male (n = 549)			Female (n = 622)			p
	Mean	SD	IQR	Mean	SD	IQR	
Follow-up interval (years)	5.00	1.58	0.86	5.13	1.52	0.88	0.1519
Δ Attenuation (HU)	-7.09	7.66	9.15	-7.45	7.85	9.45	0.4285
Δ Area (cm <sup>2</sup> )	-7.89	23.52	22.27	-4.44	17.12	15.46	0.0039
% Attenuation change	-15.98	81.43	11.95	-21.17	73.26	31.65	0.2512
% Area change	-3.25	12.76	11.51	-2.37	13.90	10.75	0.2615
Δ Attenuation (HU/year)	-1.47	2.53	1.80	-1.43	1.89	1.76	0.7577
Δ Area (cm <sup>2</sup> /year)	-2.16	11.25	4.67	-0.91	5.19	3.01	0.013
% Attenuation change/year	-0.77	71.94	4.58	-5.31	13.58	6.20	0.1231
% Area change/year	-0.92	5.41	2.39	-0.44	4.39	2.15	0.0943

HU, Hounsfield unit; IQR, interquartile range; SD, standard deviation.

Figure 4. Case of muscle tool failure due to segmentation error. (a, b) CT images in (a) soft tissue and (b) bone windows at the L3 level in a 79-year-old female show marked streak artifact related to metallic spinal fusion hardware. (c) CT scout image shows lumbar fusion and bilateral total hip arthroplasties



rate than females, though male mean muscle area was never less than that of females. As such, the male SMI was 17% higher than female SMI, which is what has been found previously in the published literature.<sup>8,17,18</sup> According to our data, after about 70 years of age, females appear to plateau more in terms of muscle bulk and density relative to males, who tend to continue dropping for both categories.

Various other studies have validated the efficacy of CT-based measurements of abdominal muscle area and attenuation, typically using manual or semi-automated methods.<sup>6-8,17-19</sup> L3 SMI is currently one of the most common measures to assess skeletal muscle quantity, using cross-sectional area ( $\text{cm}^2$ ) over patient height ( $\text{m}^2$ ) as variables. L3 SMI average values according to gender vary somewhat study by study, but normative values remain relatively similar regardless of the data gathering method, including the fully automated algorithm presented in this study (Table 3). In the existing literature, the average L3 SMI for males is  $57 \text{ cm}^2/\text{m}^2$  and for females is  $44 \text{ cm}^2/\text{m}^2$ . This study found male and female SMI to be comparable to the SMI values found in those smaller studies, which supports the validation of measurement accuracy for this fully automated method. Our results matched most closely with the largest prior study by Derstine et al,<sup>17</sup> which included 735 subjects. The slightly larger standard deviations seen in our cohort may relate to the inclusion of many non-elderly healthy adults, which would be expected to have much different measurements than older, symptomatic cohorts.

Abdominal CT is a commonly performed study on middle-age and older adults in the USA,<sup>20</sup> which provides an opportunity

to screen for multiple conditions beyond the study indication itself, such as osteoporosis, abdominal aortic aneurysm, hepatic steatosis, and metabolic syndrome.<sup>9,21-26</sup> If muscle tissue quantification is combined with other opportunistic screening tasks, such as bone mineral density, visceral fat, and aortic calcification, significant potential value may be added.<sup>9-11,27-29</sup> These additional measures can be obtained without any additional time or dose to the patient, and with relatively little or no input from the radiologist. Going forward, we plan to investigate whether these measures, including muscle bulk and density, are predictive of future adverse events, such as myocardial infarction, stroke, and death, among others. Ideally, screening for a wide variety of unsuspected conditions would help referring providers to initiate management plans for patients with concerning opportunistic screening results. Identification of such patients whose muscle mass drastically decreases over time could be useful for studying the relationship between sarcopenia and other adverse health outcomes. Furthermore, we are not aware of studies to date that have established a relationship between changes in muscle mass or attenuation and adverse clinical outcomes. This is also something we plan to investigate further.

This study has certain limitations. All cases were derived from a single medical center on asymptomatic adults employing scanners from a single CT vendor, with a fairly uniform unenhanced protocol. Although such uniformity is generally preferable when validating a new tool or approach, further external validation using a variety of different patient care settings, CT vendors, and CT techniques is warranted. We are currently assessing the impact of i.v. contrast on these muscle measures. The automated

Table 3. Comparison of SMI and SMA in adult asymptomatic screening cohort studies at L3 on CT

Study	Cohort size (n)	Mean male L3 SMI ( $\text{cm}^2/\text{m}^2$ )	Mean male L3 SMA ( $\text{cm}^2$ )	Mean female L3 SMI ( $\text{cm}^2/\text{m}^2$ )	Mean female L3 SMA ( $\text{cm}^2$ )
Graffy et al. (current study)	9310	$60.2 \pm 11.0$	$190.6 \pm 33.7$	$49.8 \pm 9.4$	$133.3 \pm 24.1$
van der Werf et al. <sup>8</sup>	420	$52.8 \pm 7.4$	$173.6 \pm 25.1$	$40.2 \pm 5.2$	$113.4 \pm 15.2$
Derstine et al. <sup>17</sup>	735	$60.9 \pm 7.8$	$195.2 \pm 25.4$	$47.5 \pm 6.6$	$128.0 \pm 17.9$
Derstine et al. <sup>18</sup>	604	$59.7 \pm 7.5$	$190.9 \pm 24.6$	$47.0 \pm 6.5$	$126.8 \pm 17.8$
Murray et al. <sup>30</sup>	50	55	$168.4 \pm 24.5$	39	$108.1 \pm 14.3$

SMI = skeletal muscle index; SMA = skeletal muscle area

tool has a finite failure rate. However, with improvements to the segmentation process, the final failure rate of the tool was <0.3%. Typically, the reason for failure was apparent by reviewing the CT images at the L3 level (Figure 4). Quality assurance for clinical use could be attained on a case-by-case basis if continued failures were to arise despite further improvements. Lastly, this initial study did not attempt to correlate muscle segmentation values with downstream adverse clinical outcomes, such as cardiovascular events, fragility fractures, and death. As mentioned, this critical next step will be the focus of future research. If we are successful in demonstrating clinical utility of this automated muscle tool in risk profiling, the next logical step would be widespread implementation as a prospective clinical tool. Utilizing this muscle tool in certain other patient care settings, such as oncology, might also prove to be quite useful. Providing an opportunistic means for earlier detection of cancer- or treatment-related wasting conditions in this vulnerable population makes sense, as this cohort often undergoes repeated CT scans for treatment response or tumor surveillance.

In summary, we provide validation for a deep learning-based automated muscle segmentation tool at abdominal CT. This automated CT tool provides both rapid and objective assessment that allowed us to apply it to a large retrospective research cohort and derive population-based normative values. We also found significant and interesting differences in both muscle area and attenuation according to gender and age. By assessing the sub cohort with longitudinal CT follow-up, this fully automated muscle segmentation method can also characterize interval changes in muscle tissue over time. With further research, it may be possible to translate this information into an opportunistic approach to evaluate sarcopenia and cachexia on any routine abdominal CT, regardless of the study indication.

## ACKNOWLEDGMENT

This research was supported in part by the Intramural Research Program of the National Institutes of Health Clinical Center and made use of the high performance computing capabilities of the NIH Biowulf system.

## REFERENCES

- Aoyagi T, Terracina KP, Raza A, Matsubara H, Takabe K. Cancer cachexia, mechanism and treatment. *World J Gastrointest Oncol* 2015; 7: 17–29p.. doi: <https://doi.org/10.4251/wjgo.v7.i4.17>
- Kim TN, Choi KM. Sarcopenia: definition, epidemiology, and pathophysiology. *J Bone Metab* 2013; 20: 1–10p.. doi: <https://doi.org/10.11005/jbm.2013.20.1.1>
- Boutin RD, Yao L, Canter RJ, Lenchik L. Sarcopenia: current concepts and imaging implications. *AJR Am J Roentgenol* 2015; 205: W255–W266p.. doi: <https://doi.org/10.2214/AJR.15.14635>
- Pahor M, Manini T, Cesari M. Sarcopenia: clinical evaluation, biological markers and other evaluation tools. *J Nutr Health Aging* 2009; 13: 724–8p.. doi: <https://doi.org/10.1007/s12603-009-0204-9>
- Goodpaster H, B., F. Thaeta, Kelley DE. *Composition of Skeletal Muscle Evaluated with Computed Tomography* 2000; 904: 18–24Vol..
- van Vugt JLA, van Putten Y, van der Kall IM, Buettner S, D'Ancona FCH, Dekker HM, et al. Estimated skeletal muscle mass and density values measured on computed tomography examinations in over 1000 living kidney donors. *Eur J Clin Nutr* 2019; 73: 879–886. doi: <https://doi.org/10.1038/s41430-018-0287-7>
- Gomez-Perez SL, Haus JM, Sheean P, Patel B, Mar W, Chaudhry V, et al. Measuring abdominal circumference and skeletal muscle from a single cross-sectional computed tomography image: A step-by-step guide for clinicians using National Institutes of health ImageJ. *JPEN J Parenter Enteral Nutr* 2016; 40: 308–18p.. doi: <https://doi.org/10.1177/0148607115604149>
- van der Werf A, Langius JAE, de van der Schueren MAE, Nurmohamed SA, van der Pant KAMI, Blauwhoff-Buskermolen S, et al. Percentiles for skeletal muscle index, area and radiation attenuation based on computed tomography imaging in a healthy Caucasian population. *Eur J Clin Nutr* 2018; 72: 288–96p.. doi: <https://doi.org/10.1038/s41430-017-0034-5>
- Pickhardt PJ, Lee SJ, Liu J, Yao J, Lay N, Graffy PM, et al. Population-based opportunistic osteoporosis screening: validation of a fully automated CT tool for assessing longitudinal BMD changes. *Br J Radiol* 2019; 92: 20180726. doi: <https://doi.org/10.1259/bjr.20180726>
- Graffy PM, Liu J, O'Connor S, Summers RM, Pickhardt PJ, et al. Automated segmentation and quantification of aortic calcification at abdominal CT: application of a deep learning-based algorithm to a longitudinal screening cohort. *Abdom Radiol* 2019; 135. doi: <https://doi.org/10.1007/s00261-019-02014-2>
- Lee SJ, Liu J, Yao J, Kanarek A, Summers RM, Pickhardt PJ, et al. Fully automated segmentation and quantification of visceral and subcutaneous fat at abdominal CT: application to a longitudinal adult screening cohort. *Br J Radiol* 2018; 65: 20170968p.. doi: <https://doi.org/10.1259/bjr.20170968>
- Pickhardt PJ. Imaging and screening for colorectal cancer with CT colonography. *Radiol Clin North Am* 2017; 55: 1183–96p.. doi: <https://doi.org/10.1016/j.rcl.2017.06.009>
- Jianhua Y, Connor SDO, Summers RM. Automated spinal column extraction and partitioning. In: *3rd IEEE International Symposium on Biomedical Imaging: Nano to Macro*; 2006.
- Burns JE, Yao J, Chalhoub D, Chen JJ, Summers RM. A machine learning algorithm to estimate sarcopenia on abdominal CT. *Acad Radiol* 2019; 21 May 2019. doi: <https://doi.org/10.1016/j.acra.2019.03.011>
- Ronneberger O, Fischer P, Brox T. *U-Net: Convolutional Networks for Biomedical Image Segmentation*, in *Lecture Notes in Computer Science*: Springer International Publishing; 2015. pp. 234–41.
- Morley JE, Anker SD, von Haehling S. Prevalence, incidence, and clinical impact of sarcopenia: facts, numbers, and epidemiology-update 2014. *J Cachexia Sarcopenia Muscle* 2014; 5: 253–9p.. doi: <https://doi.org/10.1007/s13539-014-0161-y>
- Derstine BA, Holcombe SA, Ross BE, Wang NC, Su GL, Wang SC, et al. Skeletal muscle cutoff values for sarcopenia diagnosis using t10 to L5 measurements in a healthy US population. *Sci Rep* 2018; 8: 11369p.. doi: <https://doi.org/10.1038/s41598-018-29825-5>
- Derstine BA, Holcombe SA, Goulson RL, Ross BE, Wang NC, Sullivan JA, et al. Quantifying sarcopenia reference values using lumbar and thoracic muscle areas in a healthy population. *J Nutr Health Aging* 2018;

- 22: 180–5p.. doi: <https://doi.org/10.1007/s12603-017-0983-3>
19. Kullberg J, Hedström A, Brandberg J, Strand R, Johansson L, Bergström G, et al. Automated analysis of liver fat, muscle and adipose tissue distribution from CT suitable for large-scale studies. *Sci Rep* 2017; 7: 10425p.. doi: <https://doi.org/10.1038/s41598-017-08925-8>
20. Moreno CC, Hemingway J, Johnson AC, Hughes DR, Mittal PK, Duszak R, et al. Changing abdominal imaging utilization patterns: perspectives from Medicare beneficiaries over two decades. *J Am Coll Radiol* 2016; 13: 894–903p.. doi: <https://doi.org/10.1016/j.jacr.2016.02.031>
21. Lee SJ, Pickhardt PJ. Opportunistic screening for osteoporosis using body CT scans obtained for other indications: the UW experience. *Clinical Reviews in Bone and Mineral Metabolism* 2017; 15: 128–37p.. doi: <https://doi.org/10.1007/s12018-017-9235-7>
22. Pickhardt PJ, Pooler BD, Lauder T, del Rio AM, Bruce RJ, Binkley N, et al. Opportunistic screening for osteoporosis using abdominal computed tomography scans obtained for other indications. *Ann Intern Med* 2013; 158: 588–95p.. doi: <https://doi.org/10.7326/0003-4819-158-8-201304160-00003>
23. Boyce CJ, Pickhardt PJ, Kim DH, Taylor AJ, Winter TC, Bruce RJ, et al. Hepatic steatosis (fatty liver disease) in asymptomatic adults identified by unenhanced low-dose CT. *AJR Am J Roentgenol* 2010; 194: 623–8p.. doi: <https://doi.org/10.2214/AJR.09.2590>
24. Pickhardt PJ, Hahn L, del Rio AM, Park SH, Reeder SB, Said A, et al. Natural history of hepatic steatosis: observed outcomes for subsequent liver and cardiovascular complications. *American Journal of Roentgenology* 2014; 202: 752–8p.. doi: <https://doi.org/10.2214/AJR.13.11367>
25. Pickhardt PJ, Jee Y, O'Connor SD, del Rio AM. Visceral adiposity and hepatic steatosis at abdominal CT: association with the metabolic syndrome. *AJR Am J Roentgenol* 2012; 198: 1100–7p.. doi: <https://doi.org/10.2214/AJR.11.7361>
26. Pickhardt PJ, Hassan C, Laghi A, Kim DH. CT colonography to screen for colorectal cancer and aortic aneurysm in the Medicare population: cost-effectiveness analysis. *AJR Am J Roentgenol* 2009; 192: 1332–40p.. doi: <https://doi.org/10.2214/AJR.09.2646>
27. Lee SJ, Anderson PA, Pickhardt PJ. Predicting future hip fractures on routine abdominal CT using opportunistic osteoporosis screening measures: a matched case-control study. *AJR Am J Roentgenol* 2017; 209: 395–402p.. doi: <https://doi.org/10.2214/AJR.17.17820>
28. Lee SJ, Graffy PM, Zea RD, Ziemlewicz TJ, Pickhardt PJ. Future osteoporotic fracture risk related to lumbar vertebral trabecular attenuation measured at routine body CT. *J Bone Miner Res* 2018; 33: 860–7p.. doi: <https://doi.org/10.1002/jbmr.3383>
29. O'Connor SD et al. Does Nonenhanced CT-based quantification of abdominal aortic calcification Outperform the Framingham risk score in predicting cardiovascular events in asymptomatic adults? *Radiology* 2018; 180562.